

polymer papers

Hybrids of poly(ethylene oxide-co-epichlorhydrin) and silica: phase separation, morphology and thermal properties

R. A. Zoppi* and S. P. Nunes

Universidade Estadual de Campinas, Institute of Chemistry, C. Postal 6154, CEP 13083-970, Campinas, SP, Brazil

(Revised 3 February 1998)

Hybrid materials of poly(ethylene oxide-co-epichlorhydrin), HYDRIN, and silica were prepared by a sol-gel process. An inorganic network was grown in a tetrahydrofuran/organic polymer solution from acid hydrolysis and polycondensation of tetraethoxysilane, TEOS. During solvent evaporation and simultaneous growth of the inorganic network, phase separation was observed. The mechanism of phase separation of these sol-gel systems was investigated by light scattering. Spinodal decomposition (SD) was observed for HYDRIN/TEOS systems with composition equal to 71/29, 67/33, 60/40, 50/50, 40/60, 33/67 and 29/71. The morphology of the final HYDRIN/TEOS hybrid material was investigated by scanning electron microscopy. The thermal properties of these materials were investigated by differential scanning calorimetry and their hydrophilicity was evaluated by contact angle measurements. © 1998 Elsevier Science Ltd. All rights reserved.

(Keywords: phase separation; sol-gel process; hybrids)

INTRODUCTION

The preparation and characterization of hybrid materials and their application for gas separation membranes¹ and for solid electrolytes² are subjects of current work in this laboratory. Hybrid films have been formed from mixed organic polymer/TEOS solutions. In our group, poly(methylmetacrylate), PMMA³, silicone rubber¹, poly(amide-6-*b*-ethylene oxide), PEBAX⁴, poly(ethylene oxide-co-epichlorhydrin), HYDRIN², and NAFION^{5,6} have been investigated as organic matrices. Both PEBAX and HYDRIN organic matrices originated new organic polymer/TEOS hybrid systems. In all cases, the inorganic component was grown from hydrolysis and polycondensation reactions of tetraethoxysilane, TEOS, in a solution containing the organic polymer. It is the most simple procedure to obtain hybrid films, but it can lead to a phase-separated material.

The phase separation in a multicomponent system is not always undesirable in practice. It is utilized for instance in the case of high-impact-strength polymers, where a flexible component is discontinuously embedded in a matrix of a hard component. In this particular case, phase separation between the hard and the flexible components must occur, otherwise only a plasticization effect is observed⁷. In silicone/silica hybrids, the phase separation in the nanoscale gives rise to a finely dispersed inorganic phase which hinders swelling of the polymer matrix and increases the selectivity of membranes for gas separation. Compared with HYDRIN/LiClO₄ (without silica) solid electrolytes, for HYDRIN/TEOS/LiClO₄ hybrid electrolytes², we could observe a decrease of the value of the apparent activation energy for the ionic transport. In the case of NAFION/TEOS/TMDES (TMDES = 1,1,3,3-tetramethyl-1,3-dithoxydisiloxane) hybrids^{5,6}, phase separated systems

have quite different charge transport properties with improved conductivity.

Very few studies have been published investigating the mechanism of phase separation in hybrid materials which were prepared by a sol-gel process^{3,8,9}. A large diversity of morphology can be obtained in systems which phase separate by nucleation and growth and spinodal decomposition. In this work, the phase separation in HYDRIN/TEOS (without LiClO₄) systems was investigated by light scattering measurements during the sol-gel reaction and the solvent evaporation. The final products were characterized by scanning electron microscopy, differential scanning calorimetry and contact angle measurements.

THEORETICAL CONSIDERATIONS

Phase separation is well described in the literature for polymer solutions and polymer blends^{7,10,11}. Two mechanisms are normally considered for the phase separation: nucleation and growth (NG) and spinodal decomposition (SD). The NG mechanism is preferable for quenching into the metastable phase region, between the binodal and the spinodal curves. Nucleation initiates with local density or concentration fluctuations, forming nuclei with well-defined interfaces. It requires an activation energy, which depends on the interfacial energy for creating the nuclei. The process evolution with subsequent diffusion of macromolecules into the nucleated domains is then spontaneous. The nucleus composition is constant all over the phase separation. The morphology observed during a NG phase separation is, from the early to the later stages, the droplet/matrix type. On the other hand, SD is the phase separation mechanism that predominates in quenching into the unstable region enclosed by the spinodal. Delocalized concentration fluctuations initiate spontaneously with a predominant wavelength which is constant at the very early stages and

* To whom correspondence should be addressed

depends on the quench depth. The fluctuation wavelength increases in the intermediate stages and phase coalescence is observed in the late stages. If coalescence can be avoided, a three-dimensional co-continuous morphology is obtained.

Using light scattering experiments, the NG mechanism of phase separation can be recognized by a monotonic decrease of light intensity with scattering angle. When phase separation follows the SD mechanism, a scattering halo is detected, the light intensity being maximum at a certain scattering halo.

When a phase separation follows by a SD mechanism, the linear theory proposed by Cahn and Hilliard^{12,13} can be applied at least in the early stages. Linearity is, however, expected only in the early stages of phase separation and in systems where the contribution of random thermal noise is not significant.

Considering the theory for SD, when a system reaches a condition of phase separation, the concentration fluctuations increase and the variation of concentration fluctuations, Φ (or volume fraction, φ), as a function of time, t , is described by equation (1)¹³:

$$\left(\frac{\delta\Phi}{\delta t}\right) = M\left(\frac{\delta^2 G_m}{\delta\Phi^2}\right)\nabla^2\Phi - 2Mk\nabla^4\Phi + \text{nonlinear terms} \quad (1)$$

where G_m is the free energy of mixing, M is the species mobility and k is a coefficient associated to the free energy density gradient. The concentration fluctuations can be considered as a wave and if the nonlinear terms are discarded, equation (1) have the following solution¹³:

$$\Phi - \Phi_0 = \sum_{q=0}^{\infty} \exp\{R(q)t\}\{A(q)\cos(q\delta) + B(q)\sin(q\delta)\} \quad (2)$$

where δ , A and B are constants, Φ_0 is the concentration before phase separation beginning and q is the wavenumber associated to the concentration fluctuations with wavelength Λ , as described by equation (3):

$$q = \frac{2\pi}{\Lambda} \quad (3)$$

$R(q)$ is the growth rate of the concentration fluctuations with a fixed wavenumber q and can be described by:

$$R(q) = -M\left(\frac{\delta^2 G_m}{\delta\Phi^2}\right)q^2 - 2Mkq^4 \quad (4)$$

Concentration fluctuations lead to a local heterogeneity of the refraction index, promoting the scattering of the electromagnetic radiation. $R(q)$ can be experimentally determined measuring the intensity variation of the scattered radiation as a function of time, at a fixed angle, θ . Each scattering angle can be associated to a wavenumber using equation (5):

$$q = \left(\frac{4\pi}{\lambda}\right)\sin\left(\frac{\theta}{2}\right) \quad (5)$$

where λ is the wavelength of the incident radiation.

In the early stages of the SD process, the intensity of the scattered radiation I exponentially increases as a function of time, as shown in equation (6):

$$I(q, t) \propto I(q, 0)\exp(2R(q)t) \quad (6)$$

According to equation (4), there is a critical value of the wavelength associated with the concentration fluctuations,

Λ_c , where $R(q) > 0$. By the same method, if $\Lambda < \Lambda_c$ (or $q > q_c$), $R(q) < 0$. A negative $R(q)$ means that the concentration fluctuations decrease as a function of time and they do not lead to phase separation. The theory proposes that the curve of $R(q)$ as a function of q in a SD process should have a maximum at:

$$q_m = 1/2 \left[-\frac{\left(\frac{\delta^2 G_m}{\delta\Phi^2}\right)}{k} \right]^{1/2} \quad (7)$$

or $q_m = q_c/\sqrt{2}$. The q_m value characterizes the concentration fluctuation which is predominant in the system. In practice, in a system where phase separation occurs by the SD mechanism, q_m is related to the periodical distance, d , between the two continuous phases. The periodical distance

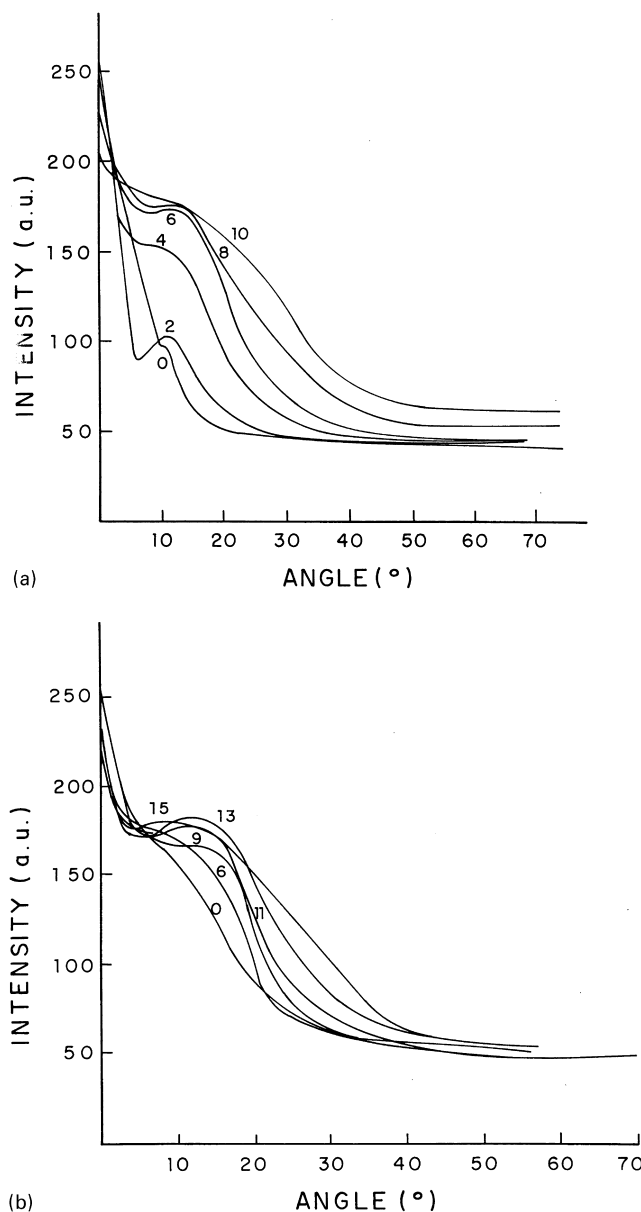


Figure 1 Evolution of scattering pattern (scattered light intensity as a function of angle) during the phase separation of: (a) 71/29; or (b) 50/50 HYDRIN/TEOS systems

Table 1 D_{ap} values for HYDRIN/TEOS systems during solvent evaporation

| HYDRIN/TEOS composition | D_{ap} (nm ² s ⁻¹) |
|-------------------------|---|
| 71/29 | 182 |
| 67/33 | 291 |
| 60/40 | 243 |
| 50/50 | 125 |
| 40/60 | 225 |
| 33/67 | 584 |
| 29/71 | 719 |

can be obtained from equation (8):

$$d = \frac{2\pi}{q_m} \quad (8)$$

According to the theory, in the early stages of the phase separation by SD, q_m does not change with the time and it can be obtained measuring the angle at which the light scattered intensity is maximum.

There is an analogy between equation (1) and the second Fick's law, in which $\delta\Phi/\delta t = D\nabla^2\Phi$, where D is the diffusion coefficient. Cahn and Hilliard proposed an apparent diffusion coefficient D_{ap} which is described by equation (9):

$$D_{ap} = -M \left(\frac{\delta^2 G_m}{\delta\Phi^2} \right) \quad (9)$$

and determined from the $R(q)/q^2$ versus q^2 curve (at $q^2 = 0$). The apparent diffusion coefficient measures the evolution of the phase separation with the time. It is zero at the spinodal curve, in which $\delta^2 G_m/\delta\Phi^2 = 0$.

EXPERIMENTAL

Sample preparation

HYDRIN was kindly supplied by Zeon Chemicals Kentucky (trade name HYDRIN C-70CG). According to the supplier information, HYDRIN C-70CG presents a glass transition temperature of -42°C , a Mooney viscosity in the range of 60–80 at 100°C , and a composition of 65 wt% of epichlorhydrin and 35 wt% of ethylene oxide (chlorine content = 25 wt%). HYDRIN was used as received.

Different volumes of tetraethoxysilane (Aldrich) were added to a continuously stirring 3 wt% HYDRIN solution in tetrahydrofuran. Drops of a 0.15 M HCl aqueous solution were then added. Usually 5 ml of solution were further stirred for 16 h at room temperature (25°C), maintained 24 h more at rest and transferred to Petri dishes with 5 cm diameter. The solvent was evaporated at normal pressure and room temperature for about 1 day and the samples were further dried under vacuum at 30°C for 1 week before final characterization.

Light scattering measurements

The equipment for light scattering measurements was mounted in the laboratory using a He–Ne laser ($\lambda = 633$ nm) as the radiation source and a photodiode as detector, which was connected to a computer by an A/D interface. A small Bosch DHP 12 V motor provided a constant variation of the detector relative to the laser. The detector angle was previously calibrated by crossing two lasers at a defined angle. The scattering pattern was recorded with the sample in a Petri dish, during the solvent evaporation at room temperature (25°C).

Table 2 Glass transition temperature ($^\circ\text{C}$) values for HYDRIN/TEOS hybrids as a function of the composition, which were obtained after different period time of the preparation

| HYDRIN/TEOS | 2 weeks | 30 weeks | 42 weeks ^a |
|-------------|---------|----------|-----------------------|
| 100/0 | -42 | -41 | -40 |
| 71/29 | -47 | -46 | -41 |
| 67/33 | -47 | -45 | -39 |
| 60/40 | -47 | -45 | -39 |
| 50/50 | -40 | -41 | -39 |
| 40/60 | -52 | -50 | -15 |
| 33/67 | -49 | -43 | -15 |
| 29/71 | -47 | -41 | -14 |

^aSamples were heated at 120°C for 1 week before the DSC measurements

Scanning electron microscopy

Samples were fractured in liquid nitrogen and coated with gold by sputtering. The fracture surfaces were observed in a JXA 840A JEOL scanning electron microscope. Samples were observed after 42 weeks of preparation.

Differential scanning calorimetry

Thermograms were obtained in a 2910 MDSC TA Instruments differential scanning calorimeter DSC. About 10 mg of sample were heated at $10^\circ\text{C}/\text{min}$ under nitrogen from -100°C up to 300°C .

Contact angle measurements

Contact angle measurements were carried out at room temperature (25°C) and 40–50% relative humidity. The drop of water was deposited on the sample with a microburette. A lens and a source light were used to create the drop image on a screen. The contact angle was determined using the projected drop image. Ten specimens of each sample were analysed. The results shown in Table 3 represent the arithmetic average followed by the standard deviation of contact angle measurements. Samples were observed after 42 weeks of preparation.

RESULTS AND DISCUSSION

Phase separation in the HYDRIN/TEOS system

Figure 1 shows the evolution of the scattering pattern during the solvent evaporation for 71/29 or 50/50 HYDRIN/TEOS systems. Similar behaviours were observed for HYDRIN/TEOS systems with other compositions. Time equal zero corresponds to the first indication of phase separation, typically near 1.5 h of solvent evaporation with an open Petri dish. During HYDRIN/TEOS hybrid formation, TEOS is initially homogeneously dispersed in the THF/HYDRIN solution. As the hydrolysis/condensation reaction goes on, the inorganic network is formed, still swollen by THF/polymer solution. The THF functions as a co-solvent swelling the growing network and diluting the unfavourable interaction between silica and organic polymer segments.

Figure 2 shows a plot of relative scattered light intensity, $I(q,t)/I(q,0)$, as a function of time for the 71/29, 50/50 and 29/71 HYDRIN/TEOS systems. Similar plots were obtained for hybrids with other compositions, confirming that when a halo was observed, the $I(q,t)/I(q,0)$ at each angle was exponential in the early stages of the process. The exponential increase is typical for spinodal decomposition. It is interesting to note that for the 40/60, 33/67 and 29/71

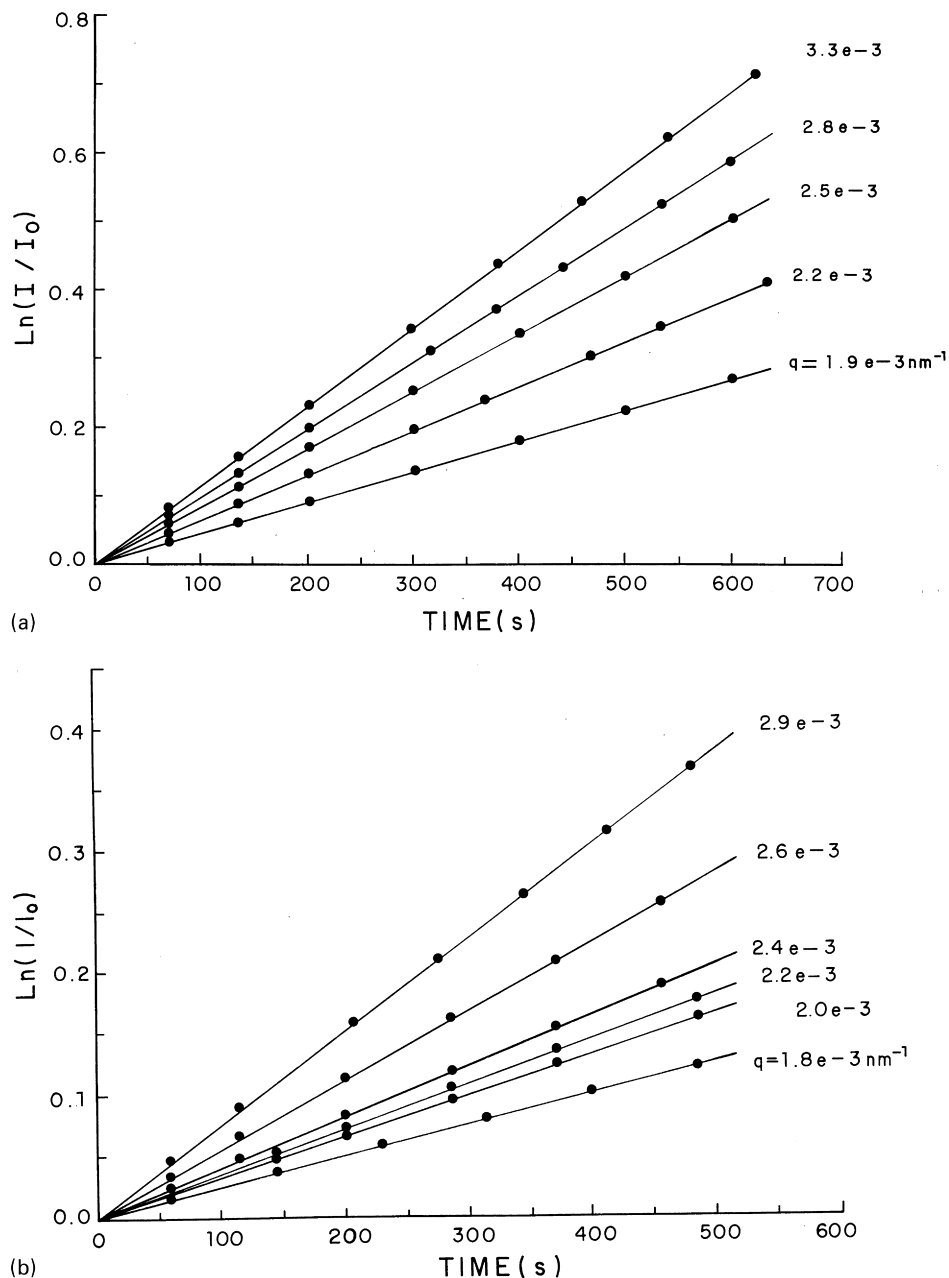


Figure 2 Relative scattered light intensity as a function of time at different angles for: (a) 71/29; (b) 50/50; and (c) 29/71 HYDRIN/TEOS systems

HYDRIN/TEOS systems the nonlinear terms in equation (1) clearly become more important as phase separation goes on. *Figure 3* shows the predominant fluctuation wavenumber as a function of time for 71/29 and 29/71 HYDRIN/TEOS systems. q_m is practically constant for hybrids with TEOS content up to 50 wt%. Above 50 wt% of TEOS, q_m decreases with time, deviating from the linear theory as an indication of coarsening. For each system, plots of $R(q)/q^2$ as a function of q^2 were obtained, as shown in *Figure 4* for the 71/29 or 67/33 HYDRIN/TEOS hybrids and apparent diffusion coefficients were determined. D_{ap} is an indication of how fast the phase separation proceeds. The D_{ap} values are shown in *Table 1* and they may be used to reflect the main differences in the system's mobility when phase separation begins. In this sense, the mobility was higher for the 29/71 HYDRIN/TEOS system. One should, however, not forget that D_{ap} has also a thermodynamic contribution and varies with the quench depth.

It is interesting to note that spinodal decomposition was

observed for all investigated compositions (from 71/29 to 29/71 HYDRIN/TEOS hybrids). These results can be better understood with the qualitative representation in *Figure 5*. Here, phase separation is induced by the solvent evaporation and simultaneous TEOS reaction. In addition to phase separation, the solvent evaporation and the reactive process may lead to gelation. There is then competition between gelation and segregation. Analogous to a phase separation process occurring by temperature variation, demixing induced by chemical reaction at constant temperature may be represented by a phase diagram in which the reaction progress is represented by an equivalent temperature, T_{eq} (relation between an attractive interaction energy and the correlation strength between monomers)³. T_{eq} decreases from infinity to low values as the inorganic polymerization reaction goes on. In *Figure 5*, the arrows indicate a combination of reaction and solvent evaporation processes. The solvent evaporation starts from a finite T_{eq} , since a considerable part of the

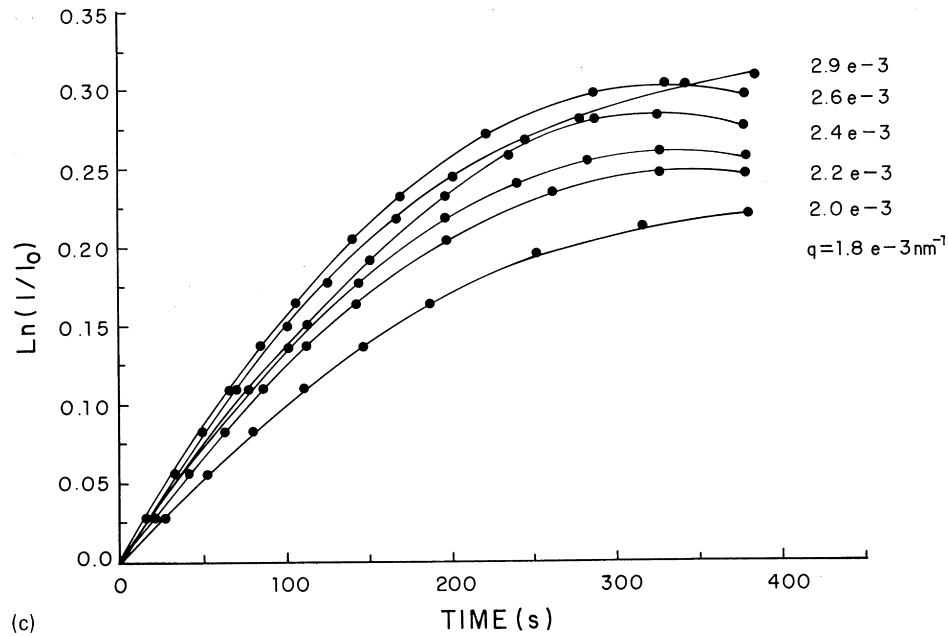


Figure 2 Continued

reaction has already taken place. ϕ is the inorganic mer concentration in the dilute medium and also varies as the solvent evaporates.

The NG is a slow rate process¹⁴. So, if the time to pass through the metastable region is short enough, phase separation by NG may not happen before the solution reaches the unstable region and begins to separate by SD mechanism. In addition, the NG mechanism is favoured when viscosity is low. In the systems investigated here, gelation and phase separation seem to happen almost simultaneously and the SD mechanism is favoured. As estimated by D_{ap} values, the mobility when SD phase separation initiated was higher for the 29/71 HYDRIN/TEOS system. For the other compositions (with less TEOS),

the system reaches the demixing condition after losing more mobility than the 29/71 hybrid, as shown by the D_{ap} values, and the gelation practically precedes phase separation curves are more separated.

Thermal analysis after solvent evaporation: aging of hybrid films

Figure 6 shows the DSC thermograms for pure HYDRIN, 60/40 and 33/67 HYDRIN/TEOS systems, which were obtained different periods of time after of the samples preparation. The transition temperature near -40°C observed for pure HYDRIN was assigned to the glass transition temperature of this elastomer. Table 2 shows the glass transition temperature for pure HYDRIN and for

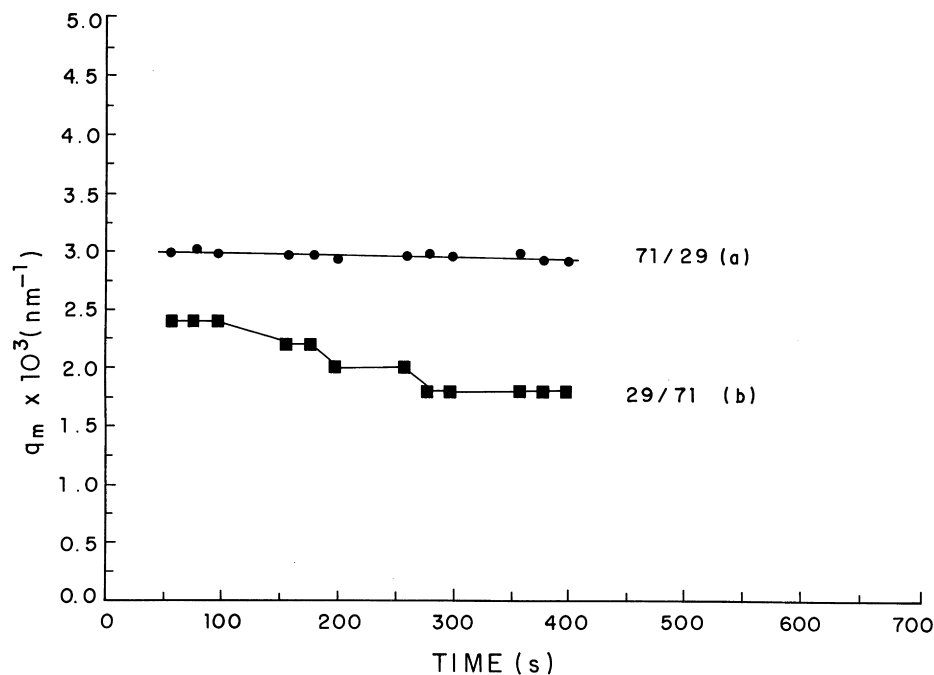


Figure 3 Wavenumber of the predominant concentration fluctuation in the system as a function of time for the: (a) 71/29; and (b) 29/71 HYDRIN/TEOS systems

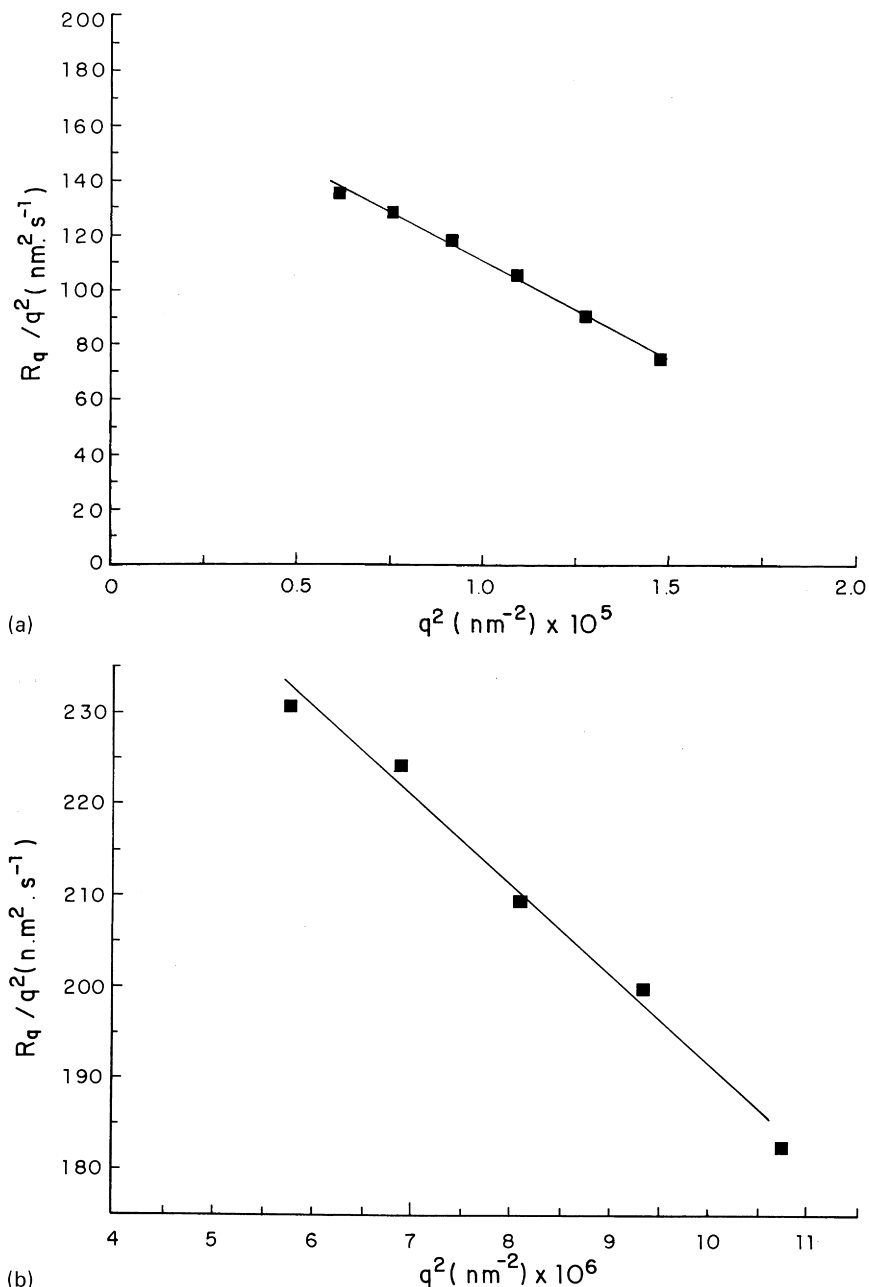


Figure 4 $R(q)/q^2$ as a function of q^2 for: (a) 71/29; or (b) 67/33 HYDRIN/TEOS systems

HYDRIN/TEOS samples obtained 2, 30 or 42 weeks after the samples preparation. Even 30 weeks after the preparation, no aging effect was observed, the T_g values practically remained constant and no variation was observed with the TEOS content. Samples were then heated at 120°C during a week and they were analysed again. After the thermal treatment, one could observe a T_g increase from -40°C to -15°C when the TEOS content was equal or higher than 60 wt%.

Comparing the T_g values obtained 2 weeks after the samples preparation, the main effect caused by the presence of the inorganic phase is an initial plasticization of the HYDRIN elastomer (T_g for hybrids is slightly lower than for pure HYDRIN, except for the 50/50 HYDRIN/TEOS system). This behaviour has been also observed in poly(methylmetacrylate)/TEOS systems and it has been assigned to presence of residual small molecules from the sol-gel reaction (for example, moieties with very low

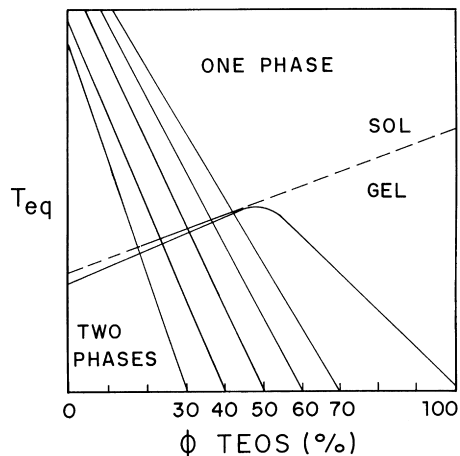


Figure 5 Qualitative representation of the phase diagram of HYDRIN/TEOS system

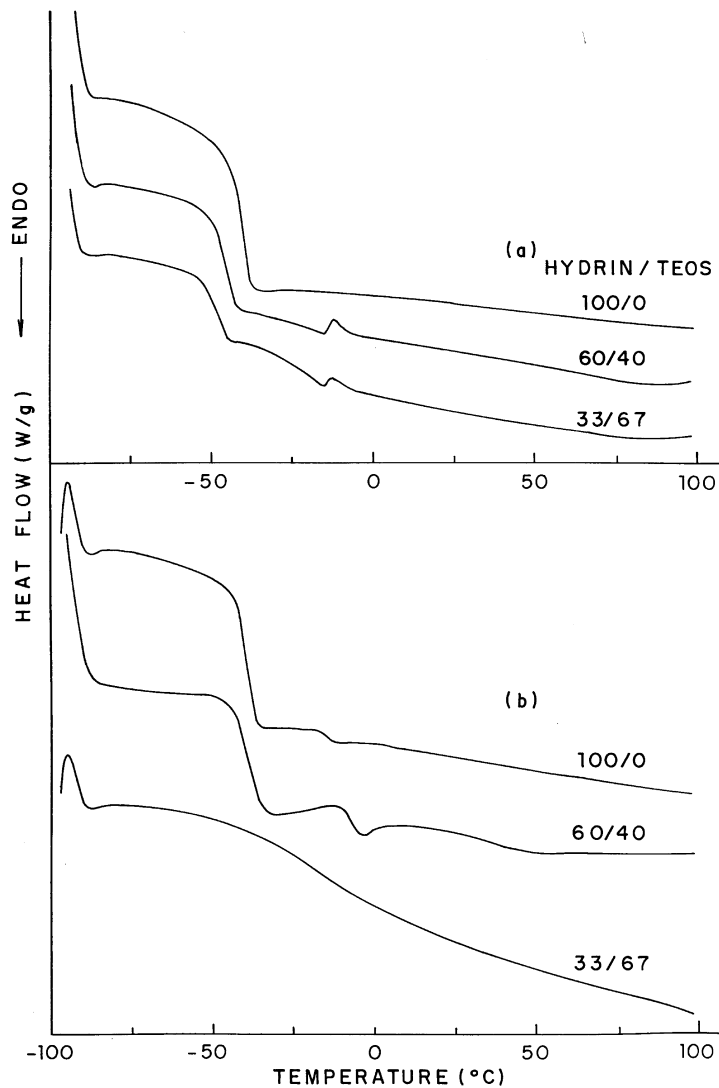


Figure 6 DSC thermograms for pure HYDRIN and HYDRIN/TEOS systems obtained: (a) 2; or (b) 42 weeks after the samples preparation. In case (b), samples were heated at 120°C for 1 week before the DSC measurements

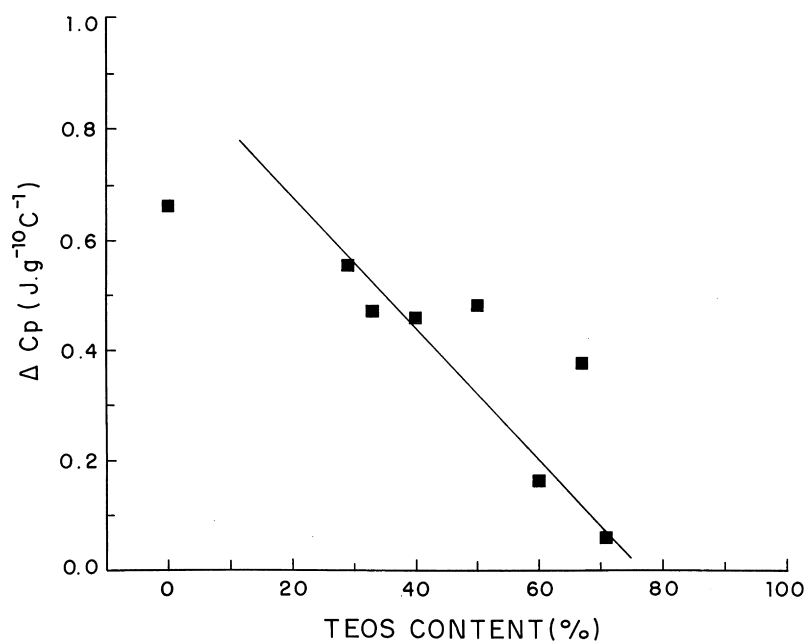


Figure 7 ΔC_p as a function of TEOS content for HYDRIN/TEOS systems. Samples were heated at 120°C for 1 week before the DSC measurements, which were carried out 42 weeks after the samples preparation

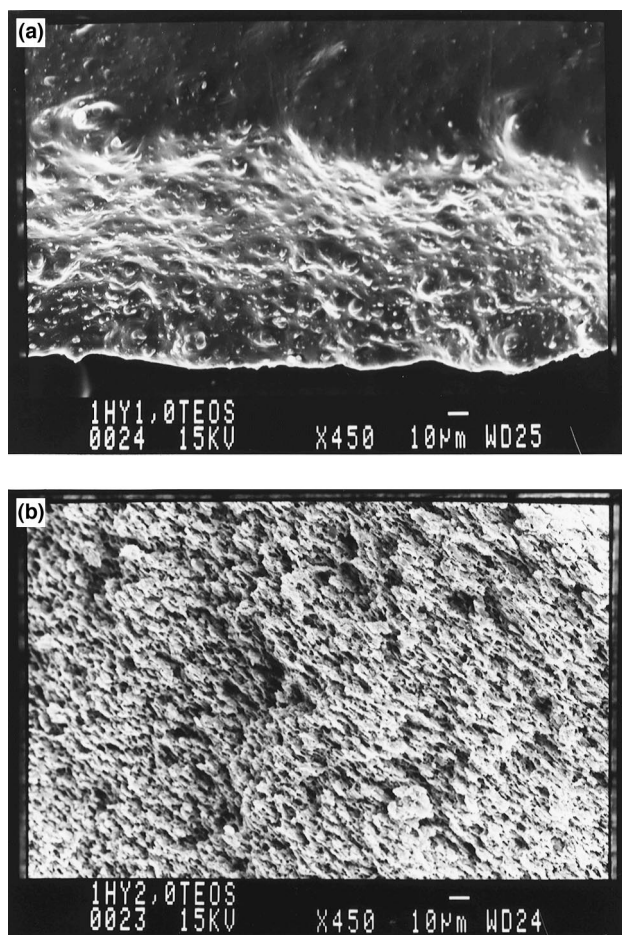


Figure 8 Scanning electron microscopy of: (a) 50/50; and (b) 33/67 HYDRIN/TEOS systems

Table 3 Contact angle values for HYDRIN/TEOS hybrids as a function of the composition

| HYDRIN/TEOS composition | Contact angle (°) |
|-------------------------|-------------------|
| 100/0 | 129 ± 3 |
| 71/29 | 130 ± 4 |
| 67/33 | 126 ± 7 |
| 60/40 | 123 ± 3 |
| 50/50 | 116 ± 3 |
| 40/60 | 113 ± 2 |
| 33/67 | 106 ± 1 |
| 29/71 | 107 ± 2 |

degrees of polymerization such as monomers and dimers), indicating incomplete curing of the inorganic phase¹⁵. When the measurements were carried out 30 weeks after the samples preparation, no significant variation was observed. Only after submitting the samples to a thermal treatment, a T_g variation with the TEOS content could be verified, as shown in *Table 2*. As expected, an increase in the TEOS content promoted a hardening effect of the elastomer.

It is interesting to consider the variation of the heat capacity (Δcp) during the glass transition as a function of TEOS content. *Figure 7* shows that Δcp linearly decreases with the increase of TEOS content in the hybrids. The Δcp variation as a function of the composition of a multi-component system can be used to indicate the existence of interactions between the components. In systems where no interaction exists, the additivity of free volume is expected and a linear behaviour of Δcp as function of composition shall be verified¹⁶, as it was observed for HYDRIN/TEOS

systems. Δcp is also related to the magnitude of the glass transition, which decreased with the increase of TEOS content, as shown in *Figures 6* and *7*. The molecular movements of the organic amorphous chains suffer restrictions imposed by the rigid inorganic phase.

Morphology

Figure 8 shows the morphology observed by scanning electron microscopy for 50/50 or 33/67 HYDRIN/TEOS hybrids. For hybrids with a TEOS content up to 50 wt%, the matrix seems to be elastomeric, rich in HYDRIN. 50 wt% TEOS leads to 23 wt% inorganic phase in the hybrid, which forms the disperse domains in *Figure 8*. In hybrids with higher TEOS content, as shown in *Figure 8* for a hybrid with 67 wt% TEOS (37 wt% SiO₂), the inorganic component forms a continuous phase.

Contact angle measurements

Contact angles are sensitive to surface modifications occurring at a depth of 20–30 Å^{17,18}.

Table 3 shows the contact angle for HYDRIN/TEOS hybrids as a function of TEOS content. When the TEOS content increased, the surface became less hydrophobic, as indicated by the contact angle decrease. The increase of TEOS content probably promotes an increase of -OH groups on the film surface, also increasing the hydrophilicity.

CONCLUSIONS

The phase separation of HYDRIN/TEOS hybrids was investigated by light scattering, during simultaneous solvent evaporation and hydrolysis/polycondensation of TEOS. All the investigated systems, containing 29–71 wt% TEOS (relative to HYDRIN content), demix by the spinodal decomposition and the results follow the linear Cahn theory. For systems with TEOS content higher than 60 wt% the non-linear terms of this theory become more important. Systems with high TEOS content have higher mobility (high D_{ap} values) and, in the later stages of phase separation, coarsening can be detected with a consequent shift of q_m , the predominant concentration fluctuation. The morphology of the final hybrids was investigated by scanning electron microscopy. In hybrids with TEOS content below 50 wt%, the matrix is clearly rich in elastomeric component and the inorganic phase is dispersed as domains. Above 50 wt% TEOS, the inorganic phase is continuous. No aging was detected by thermal analysis in systems stored at room temperature (25°C), under vacuum, and after 30 weeks of the preparation.

ACKNOWLEDGEMENTS

The authors thank FAPESP (Proc. 94/2161-9 and 95/3636-3) and CNPq for financial support.

REFERENCES

1. Nunes, S. P., Schultz, J. and Peinemann, K. V., *J. Mater. Sci. Lett.*, 1996, **15**, 1139.
2. Zoppi, R. A., Fonseca, C. M. N. P., De Paoli, M.-A. and Nunes, S. P., *Acta Polym.*, 1997, **48**, 131.
3. Silveira, K. F., Yoshida, I. V. P. and Nunes, S. P., *Polymer*, 1995, **36**, 1425.
4. Zoppi, R. A., Castro, C. R., Yoshida, I. V. P. and Nunes, S. P., *Polymer*, 1997, **38**, 5705.
5. Zoppi, R. A., Yoshida, I. V. P. and Nunes, S. P., *Polymer*, 1997, **39**, 1309.

6. Zoppi, R. A. and Nunes, S. P. J., *Electroanal. Chem.*, 1998, **445** (1–2), 39.
7. Elias, H. G., *Macromolecules*, Vol. 1. Plenum Press, New York, 1977.
8. Nakanishi, K. and Soga, N., *J. Non-Crystalline Solids*, 1992, **139**, 1.
9. Nakanishi, K. and Soga, N., *J. Non-Crystalline Solids*, 1992, **139**, 14.
10. Inoue, T. and Ougizawa, T., *J. Macromol. Sci.-Chem.*, 1989, **A26**, 147.
11. Utracki, L. A., *Polymer Alloys and Blends*. Hanser, Munich, 1990.
12. Cahn, J. W., *J. Chem. Phys.*, 1965, **42**, 93.
13. Cahn, J. W. and Hilliard, J. E., *J. Chem. Phys.*, 1958, **28**, 258.
14. Inoue, T., Ougizawa, T., Yasuda, O. and Miyasaka, K., *Macromolecules*, 1985, **18**, 2089.
15. Landry, C. J. T., Coltrain, B. K. and Brady, B. K., *Polymer*, 1992, **33**, 1486.
16. Cassu, S. N. and Felisberti, M. I., *Polymer*, 1997, **38**, 3907.
17. Fadda, E., Berenguer, M. and Clarisse, C., *J. Vac. Sci. Technol.*, 1995, **B13**, 1055.
18. Kano, Y. and Akiyama, S., *Polymer*, 1993, **34**, 376.